Nonlinear Broadband Wave Energy Harvesting via Pendulum-Based Converters for Sustainable Self-Powered Marine Observation: A Review

Jiaze Kou, Qijian Feng and Tiancong Zhao*

Zhuhai Campus, Beijing Institute of Technology, Zhuhai 519088, P. R. China

Abstract: Pendulum-based wave energy converters (WECs) offer a promising route to self-powered marine observation. A sealed buoy converts low-frequency, irregular, and multidirectional wave motion into electricity for onboard sensors and telemetry, reducing battery-replacement and vessel-access requirements. This review synthesizes evidence in four groups: built-in and miniaturized point absorbers, rotating-pendulum electromagnetic harvesters, triboelectric nanogenerators (TENGs), and hybrid TENG–electromagnetic systems. The first two groups define the core pendulum-based scope; TENG and hybrid studies without a pendulum are included only as contextual comparators when they inform low-frequency conversion, power management, durability, or marine deployment. Rather than cataloguing devices, the review groups them by nonlinear mechanism, with emphasis on parametric excitation, rotational orbits, multistability, and bounded chaos, which can broaden the operating bandwidth under realistic sea states. On that mechanistic basis, a fluid–mechanical–electrical coupled modeling framework is outlined, together with design principles, experimental standardization, and field-validation requirements for self-powered observation buoys. Because progress is constrained less by isolated peak outputs than by the incompatibility of reported metrics, the review also sets out minimum reporting requirements for cross-study comparison. It then assesses remaining challenges in power-take-off design, energy management, durability, and the sustainability of distributed ocean observation. Together, these strands indicate how miniature pendulum WECs may move from laboratory prototypes toward energy-autonomous marine sensing infrastructure, while identifying where the evidence remains too thin to support that transition.

Keywords: Pendulum wave energy converter, self-powered marine observation, nonlinear dynamics, broadband energy harvesting, triboelectric nanogenerator, marine renewable energy.

1. INTRODUCTION

Sustained ocean observation underpins weather forecasting, climate services, ecosystem protection, hazard warning, and offshore operations. Yet the density and persistence of observations remain constrained by battery replacement, vessel access, and the power demand of sensing and communication hardware [1-6]. Energy autonomy therefore links marine renewable energy directly to the sustainability goals of the United Nations Decade of Ocean Science: a buoy that harvests locally and schedules its own measurements can reduce maintenance voyages, disposable batteries, and observation gaps.

Ocean waves offer high availability and spatial reach, but their motion is low-frequency, irregular, multidirectional, and intermittently energetic. Conventional wave energy converters are optimized for grid-scale power and are often too large or maintenance-intensive for distributed instruments [7-12]. In contrast, a built-in WEC packages the moving mechanism and power take-off (PTO) inside a sealed hull, protecting active parts while preserving the external form of a buoy, drone, or navigation aid [13-14]. For sensor-scale harvesting, spectral targeting also differs from utility-scale conversion: the higher-frequency tail of the wave spectrum can be attractive because smaller devices can access it without reproducing the dominant-wave resonance of a large hull [15].

Pendulum converters are well suited to this scale separation. Wave-induced surge, sway, heave, roll, pitch, and yaw are transformed into relative pendulum motion and then into electrical output through electromagnetic generators (EMGs), triboelectric nanogenerators (TENGs), or hybrid PTOs. Their central difficulty is also their scientific opportunity: a linear pendulum responds strongly only near resonance, whereas real seas continually shift the excitation amplitude, direction, and frequency. Parametric instability, rotation, multistability, magnetic softening, impact, and bounded chaos can enlarge the usable response domain when the nonlinear dynamics and electrical loading are co-designed rather than treated as parasitic effects [16-28].

This review connects three bodies of work that are frequently discussed separately: floating-system architecture, nonlinear pendulum dynamics, and low-power marine instrumentation. To keep the comparisons interpretable, it distinguishes core pendulum-based converters, related pendulum-coupled hybrids, and contextual non-pendulum TENG/EMG systems. Only the first two categories are used to infer trends specific to pendulum WECs; contextual systems are used to benchmark conversion, power management, durability, and marine

*Address correspondence to this author at the Zhuhai Campus, Beijing Institute of Technology, Zhuhai 519088, P. R. China; E-mail: zhaotc@bit.edu.cn

Received on 09-10-2026 Accepted on 17-11-2026 Published on 20-11-2026

E-ISSN: 3083-0850/26

integration. Section 2 compares representative systems using two quantitative tables. Section 3 explains the mechanisms that create broadband response and the role of electromechanical damping. Section 4 presents a coupled design framework, reporting checklist, and sustainability perspective for moving from laboratory prototypes to self-powered observation systems. The emphasis is not peak voltage alone, but net stored energy, sensing availability, deployment reliability, and lifecycle value.

2. PENDULUM-BASED AND HYBRID FLOATING WECS: STATE OF THE ART

2.1. Point Absorbers and Built-in Converters

A floating point absorber converts the relative motion between a body and a reference into useful work. At observation-buoy scale, the hull itself supplies the inertial excitation while the reference is created internally by a pendulum, proof mass, liquid column, or gyroscope. This built-in arrangement avoids exposed linkages and allows the same pressure boundary to protect the generator, bearings, power electronics, and battery. The trade-off is strong internal coupling: the moving mass shifts the center of gravity, changes roll and pitch natural periods, and can increase mooring loads. Recent reviews therefore treat hull, internal converter, PTO, and mooring as a single system rather than sequential subsystems [13-14,29]. The power requirements of representative ocean-sensing platforms are illustrated in Figure **1**.

Rigid-hull encapsulation is particularly useful for autonomous platforms because exterior geometry can be optimized for hydrodynamics and survivability while the converter remains modular. However, device size should not be reduced by geometric scaling alone. Viscous losses, bearing friction, Coulomb friction, cable torque, generator cogging, and battery-converter thresholds become proportionally larger at small scale, whereas captured hydrodynamic power decreases rapidly. Application-led sizing begins with the sensor duty cycle and daily energy budget, then selects hull motion modes and a conversion mechanism capable of delivering charge above the storage threshold under representative sea spectra. Figure **2** provides an overview of several types of wave energy converters. This section focuses on built-in designs in which the moving mechanism and power take-off are enclosed within the floating hull. Representative internal converter arrangements within rigid floating hulls are shown in Figure **3**.

Integration with coastal structures is another route to increased value. A pendulum-WEC array coupled to a floating breakwater was reported to increase power output by up to 397% while reducing wave transmission and pitch-related mooring force, although the gains depend on spacing, wave direction, and scale

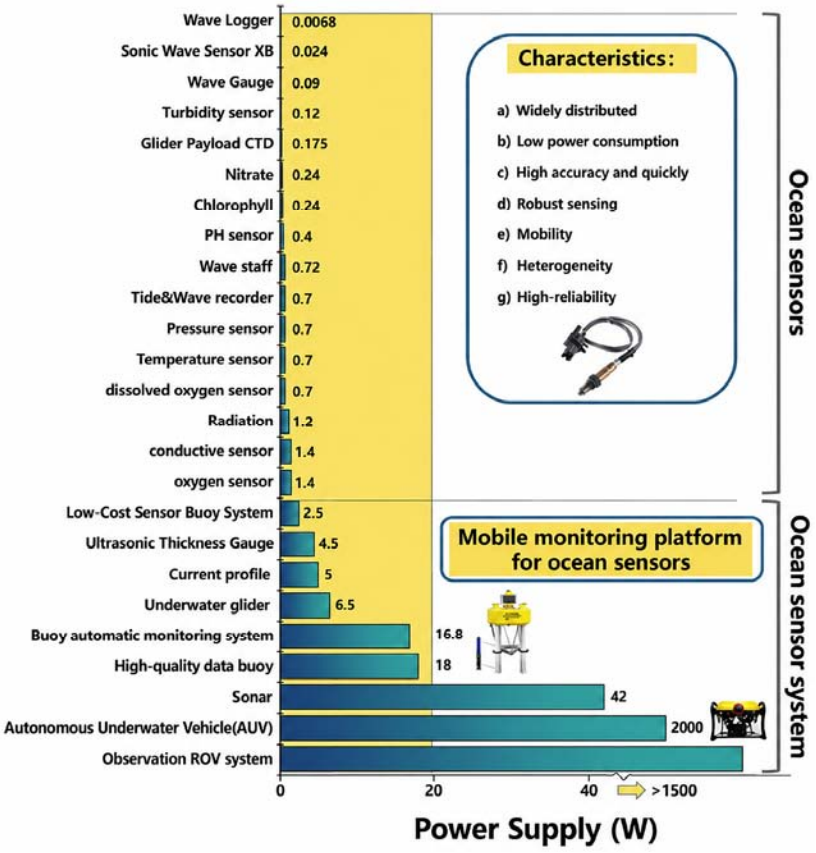


Figure 1: Representative power requirements of ocean-observation platforms. Sources: Refs. [2-6].

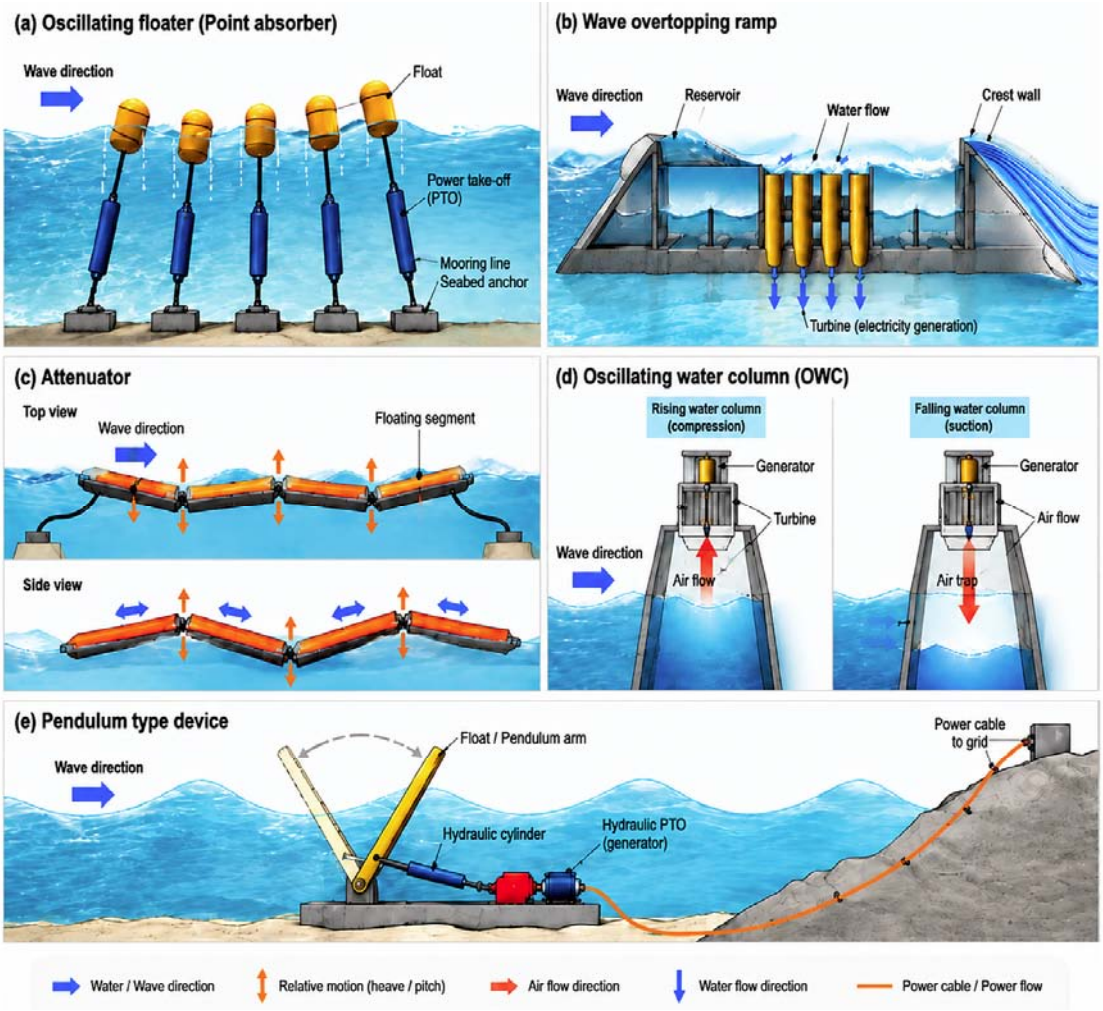


Figure 2: Operating principles of several types of wave energy converters.

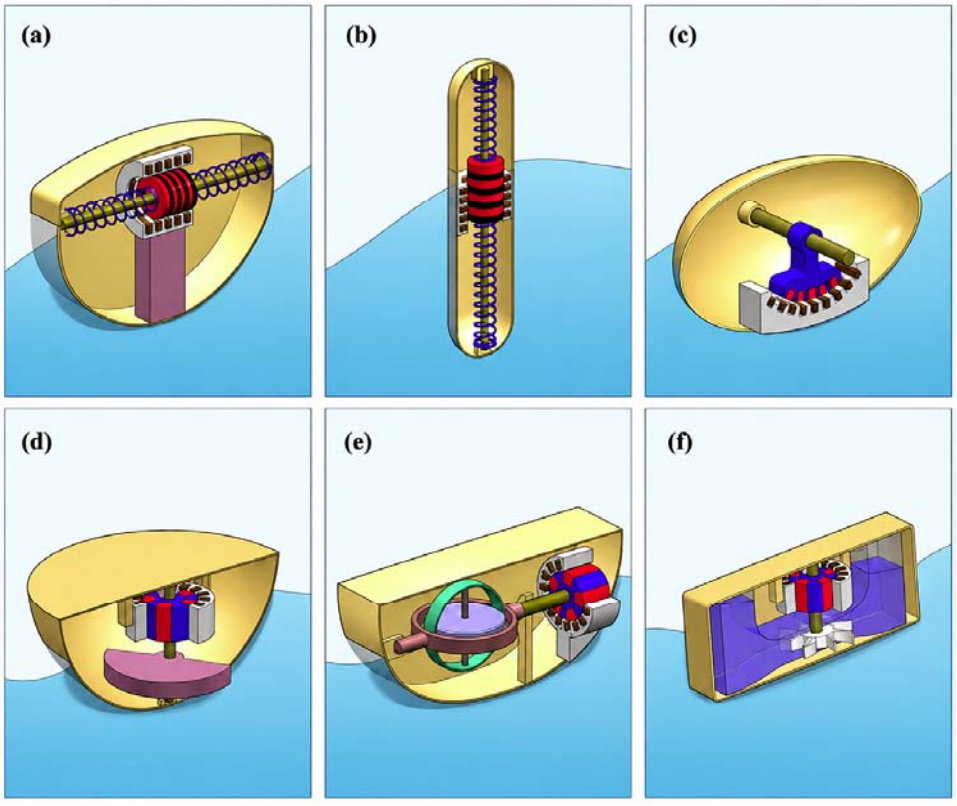


Figure 3: Typical built-in converter arrangements within rigid floating hulls. Source: Ref. [13].

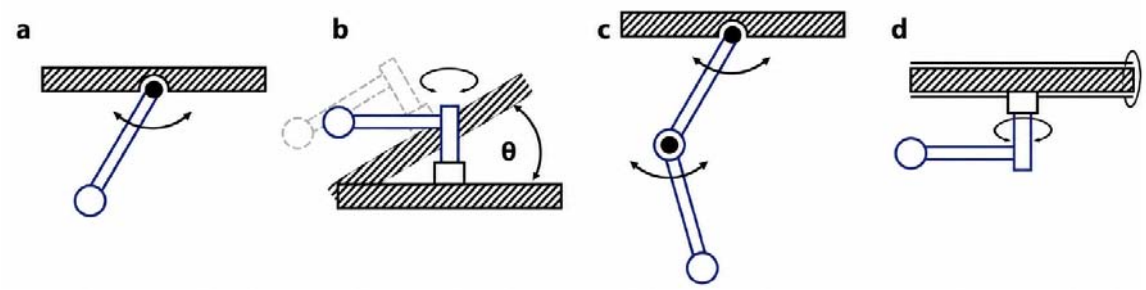


Figure 4: Single-axis eccentric pendulum and electromagnetic PTO concept.

[30]. Similar multifunctionality can couple observation, navigation, aquaculture, or autonomous-vehicle missions to energy harvesting without requiring a stand-alone energy device.

2.2. Rotating-Pendulum Electromagnetic Harvesters

Single-axis eccentric pendulums remain the simplest electromagnetic architecture. A wave-excited hull rotates the pendulum relative to the enclosure, and a gear train or direct-drive rotor converts angular motion into generator speed. Guo *et al*. introduced an eccentric-sector device with speed multiplication, while Li *et al*. developed a sealed swing-body harvester for an ocean buoy [31,32]. These mechanisms are compact and mechanically transparent, but their response is directional and their gear trains add backlash and friction. The single-axis eccentric pendulum coupled to an electromagnetic PTO is illustrated in Figure **4**.

Axis orientation is a design variable. Jiang *et al*. evaluated a vertical-axis pendulum within a hemispherical float and reported a capture-width ratio of approximately 0.39 [33]. Ding *et al*. instead used a horizontal pendulum mounted on a pitch-adjustable bottom plate inside an underwater mooring platform. In their tests, pitch angles of 3°, 4°, and 5° placed the resonant frequency at 0.2, 0.25, and 0.3 Hz, so a small tilt keeps the resonance in the low-frequency band and allows it to be matched to the dominant excitation of the platform [34]. Tilting can activate direct and parametric excitation within the same mechanism, but it also complicates the coupling between platform attitude and pendulum motion. The two configurations are shown in Figure **5**.

Two single-pendulum arrangements set the reference point for the rest of this section. The first is the ballasted horizontal pendulum described above, sealed inside an underwater mooring platform [34]. The second is an eccentric pendulum rotor, whose rim magnets act as both field source and eccentric mass so that a thin horizontal-coil rotor reaches the low-frequency band without gears [35]. Multi-pendulum variants, by contrast, add degrees of freedom and can exploit chaotic motion, but both studies remain at bench or numerical level [36,37]. Both arrangements are narrowband, which is why tuning is treated as a design requirement in Section 3. The two configurations are compared in Figure **6**.

Beyond the single-pendulum designs in Figure **6**, Figure **7** shows laboratory double-pendulum systems for chaotic energy harvesting [36] and magnetic-interaction studies [37]. For multidirectional harvesting, Wang and Lee used orthogonal eccentric

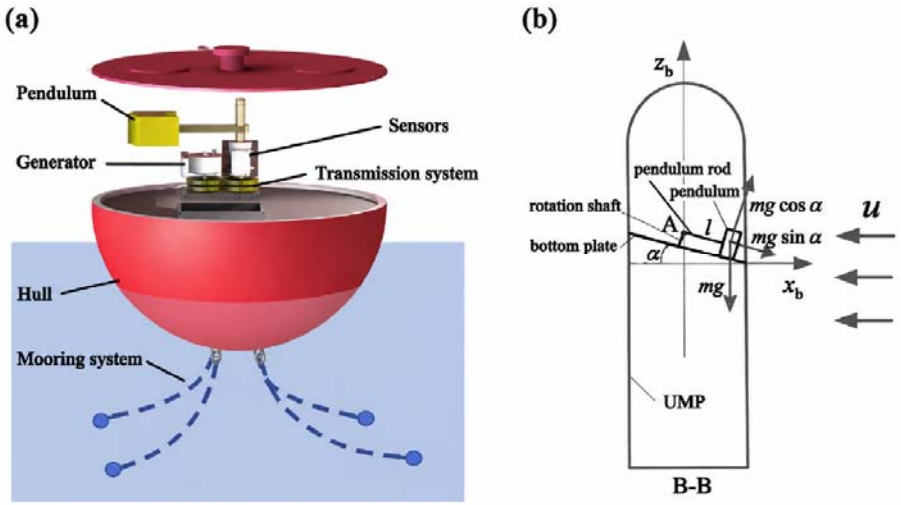


Figure 5: Vertical-axis pendulum converter in a hemispherical floating hull and pitch-adjustable horizontal pendulum for an underwater mooring platform. Sources: Refs. [33,34].

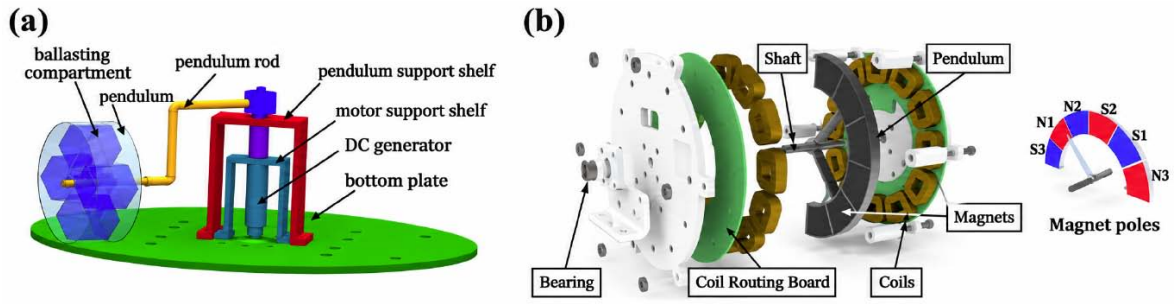


Figure 6: Ballasted horizontal pendulum for an underwater mooring platform and eccentric magnet-rotor electromagnetic harvester. Sources: Refs. [34,35].

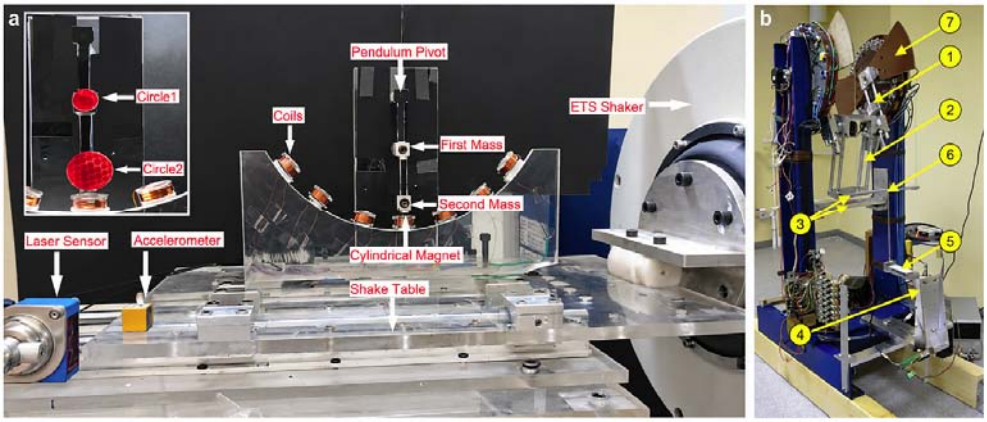


Figure 7: Laboratory double-pendulum systems for nonlinear dynamics and energy-harvesting studies. Sources: Refs. [36,37].

rings that mimic biaxial hula-hoop motion and generated power at buoy-motion frequencies of 0.7–1.0 Hz [38]. This biaxial configuration is shown in Figure **8**. The WITT concept uses a compound pendulum whose rotation about two perpendicular horizontal axes is transferred through a gearbox to a single output [39]. Its configuration is illustrated in Figure **9**. Gyroscopic converters provide another approach, although rotor-spin and control power must be included in the net energy balance [40].

Table **1** links studies of pendulum dynamics and floating converter response with prototype development and platform integration. Multi-axis designs can use motion about more than one axis [38,39], while resonance tuning and adjustable PTO damping can help converters respond to changing wave excitation [28,42]. Most experimental evidence comes from bench and wave tank tests. Li *et al*. [32] reported electrical output during a sea trial, but evidence of sustained operation at sea remains limited among the studies listed. For marine deployment, generator efficiency should be assessed together with the converter's dynamic response and its interaction with the mooring system [45].

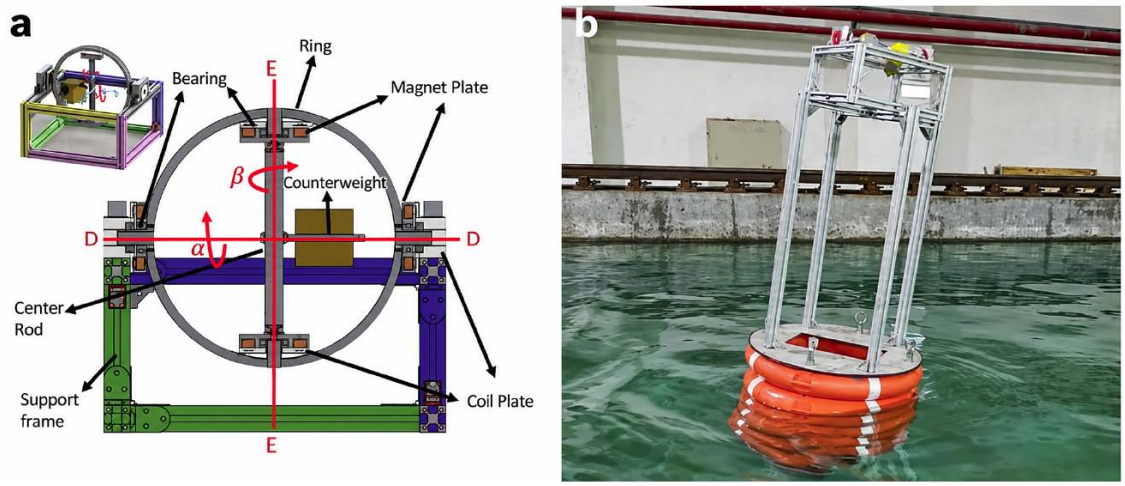


Figure 8: Biaxial hula-hoop pendulum converter for a mooring-less buoy. Source: Ref. [38].

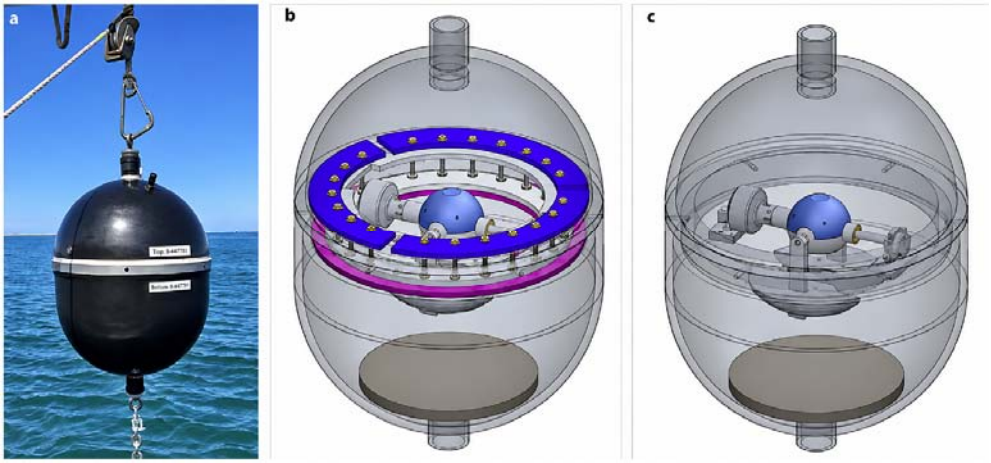


Figure 9: WITT wave energy converter and its compound-pendulum transmission. Source: Ref. [39].

Table 1: Representative Studies on Pendulum-Based Wave Energy Conversion and Related Technologies

Study	Configuration and PTO	Test or validation	Reported performance	Salient feature or limitation	Ref.
A. Electromagnetic harvester prototypes					
Guo *et al.* (2018)	Eccentric sector pendulum and geared EMG	Wave flume prototype test	122 mW estimated at 20 m/s wind speed	Gearing increases generator speed	[31]
Li *et al.* (2019)	Rotating pendulum and geared EMG	Yellow Sea field trial	Up to 0.13 W at peak wave heights >0.6 m	Targets ultra-low frequency; sealed buoy	[32]
Wang and Lee (2019)	Orthogonal biaxial eccentric rings; drifting buoy	Wave flume test	0.56 W at 0.7–1.0 Hz buoy motion	Unmoored buoy	[38]
Shalaby *et al.* (2025)	Sensing buoy with pendulum, AC generator, and rectifier	Wave tank test of a 1:8.5 model	n.r.	Designed for met-ocean sensing	[43]
B. Dynamics and modeling of floating converters					
Jiang *et al.* (2023)	Vertical-axis pendulum in a hemispherical float	Scaled basin tests and modeling	Modeled max. CWR: 39.05%	Basin tests evaluated pendulum motion	[33]
Crowley *et al.* (2018)	WITT compound pendulum and gearbox	Numerical model and wave tank tests	Mechanical response validated	No PTO installed in the wave tank model	[39]
Jiang *et al.* (2025)	Vertical-axis pendulum in a rigid hull	Perturbation and simulation	Predicted annual yield: ≈6.79 MWh	Mounting above the hull mass center favored	[41]
C. Pendulum response and resonance tuning					
Lenci *et al.* (2012)	Parametric pendulum on water waves	Wave-flume experiment	n.r.	Early water-wave rotation demonstration	[21]
Yurchenko and Alevras (2018)	Parametric pendulum under stochastic base excitation	Bench and stochastic analysis	n.r.	Rotating solutions under random input	[24]
Reid *et al.* (2024)	Multiple orientations; surge, heave, dynamic tilt	Theory and experiment	12.5 W peak (heave); ~1 W (dynamic tilt)	Quantifies bandwidth–peak-power trade-off	[25]
Ding *et al.* (2016)	Pitch-adjustable horizontal pendulum	Laboratory roll excitation	Pitch angle shifts the peak-power frequency	For underwater mooring platforms	[34]
Kumar *et al.* (2019)	Horizontal-axis chaotic double pendulum	Modeling and bench tests	n.r.	Chaotic motion used for energy harvesting	[36]
Wojna *et al.* (2018)	Double physical pendulum with magnetic interaction	Numerical and experimental	n.r.	Nonlinear magnetic coupling; multiple responses	[37]
D. PTO control and platform integration					
Huang *et al.* (2025)	Pendulum-WEC array with floating breakwater	Numerical optimization and flume	Power +397% (max.); transmission −73%; pitch mooring force −75%	Multifunctional structure; layout-sensitive	[30]
Gu *et al.* (2025)	Digitally controlled variable-area hydraulic PTO	Prototype and co-simulation	+37.04% captured energy; ~95% average mechanical efficiency	Real-time PTO damping adaptation	[42]
Khan *et al.* (2025)	Pendulum WEC in an ocean drone keel	Wave tank prototype test	n.r.	PTO type unspecified in the public abstract	[44]

Notes: n.r., not reported or not quantified in the source available for verification; CoG, center of gravity. Power and output are quoted as reported. Differences in scale, regularity, wave amplitude, excitation type, and load prevent direct ranking across studies.

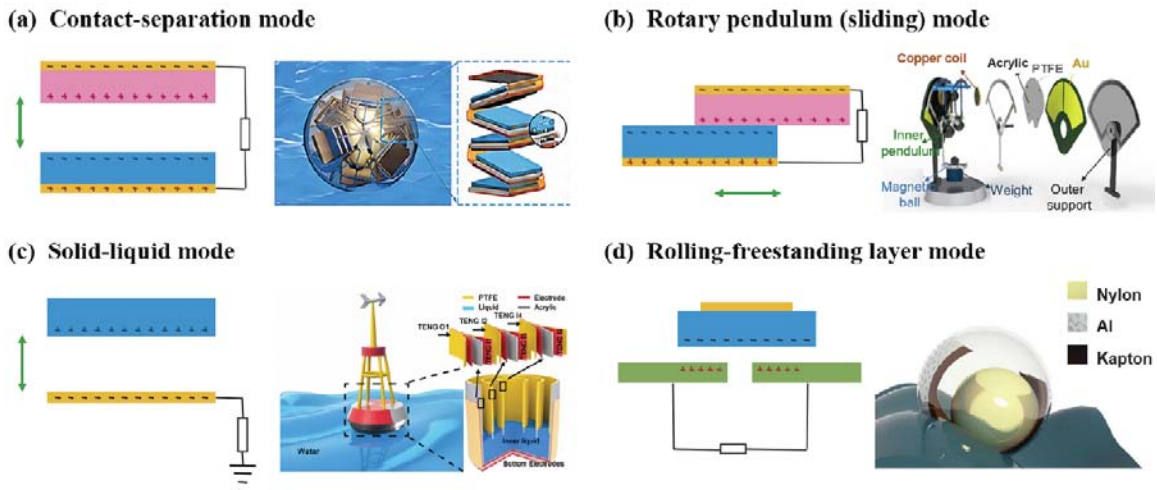


Figure 10: Simplified operating schematics and representative configurations of triboelectric nanogenerators for water-wave energy harvesting. Sources: Refs. [48,59,64,79,81].

2.3. TENG-Based Harvesters

TENGs convert periodic contact, separation, sliding, or rolling into high-voltage alternating output through contact electrification and electrostatic induction [46-52]. Their low-frequency sensitivity, light moving elements, and modular electrodes fit small buoys, but their high internal impedance makes load matching and rectification decisive. Water-wave devices include rolling spheres, tower-like stacks, swing cylinders, folded membranes, and liquid–solid interfaces [53-77]. Unless a pendulum or pendulum-like swing element is explicitly present, these studies are used as contextual comparators rather than as evidence for pendulum-specific performance. Figure **10** pairs simplified operating schematics with representative TENG devices for water-wave energy harvesting. These examples illustrate how relative motion and changing interfacial contact induce charge transfer.

For an autonomous node, open-circuit voltage is not a sufficient performance measure. The relevant chain is rectified charge, conversion efficiency, storage gain, quiescent loss, and useful load energy over a sea-state distribution. Mechanical durability must also be reported because contact wear, particle contamination, humidity, and encapsulation leakage can progressively change surface charge. Designs using rolling or soft contact reduce abrasion, whereas charge-excitation and opposite-charge-enhancement circuits increase charge density at the cost of additional circuitry [63,69,70,75,78-83].

2.4. Hybrid TENG–EMG Systems

Hybrid TENG–EMG systems exploit complementary electrical characteristics. The EMG supplies comparatively high current and average power when rotational speed is adequate, whereas the TENG supplies high voltage and remains responsive at low frequency. A common moving element can drive both transducers, limiting package size and enabling a shared rectifier-storage stage. Early devices ranged from enclosed rolling hybrids to chaotic-pendulum and soft-contact swing mechanisms [84-96]. In this review, hybrids without a pendulum are retained as contextual comparators because they provide useful evidence on rectification, storage, durability, and marine integration.

Recent designs increasingly integrate mechanical rectification, gearing, and sensing. A bidirectional turbine–planetary-gear harvester maintained operation at 0.25 Hz; its reported peak outputs were 115 mW for the TENG and 350 mW for the EMG, corresponding to volume-normalized peak densities of 32.55 and 329.78 W/m³, respectively [97]. Because this turbine-based device has no pendulum, it is used here as a contextual comparator. Pressure-driven and gyroscopic hybrids extend the response to oscillating-water-column and omnidirectional-current inputs [98,99]. A chaotic pendulum with a tower-integrated TENG–EMG and charge-excitation circuit achieved frequency-normalized peak power densities of 56.7 and 192.3 W/(m³·Hz), followed by water-tank and open-sea demonstrations [100]. These figures are study-specific benchmarks rather than a universal ranking because the normalization basis, excitation conditions, and electrical loads differ. A broadband hybrid blue-energy nanogenerator has also been proposed for smart ocean IoT networks [101]. Table **2** compares the architectures, test conditions, output metrics, and demonstrated loads of representative TENG-based and hybrid systems, with non-pendulum entries treated as contextual comparators.

The comparison suggests that hybridization is most valuable when evaluated at the storage interface. EMG current can reduce charging time, while TENG voltage can activate low-energy events and sensing functions. The 400,000-cycle and 2.33-million-cycle results come

Table 2: Contextual Comparison of TENG-Based and Hybrid Marine Energy Harvesters Relevant to Self-Powered Observation

Study	Type	Architecture	Test condition	Reported output or evidence metric	Demonstrated load or feature	Ref.
Xu *et al*. (2019)	TENG	Tower-like; PTFE balls on arc nylon films	Laboratory	1.03 to 10.6 W/m³ for 1 to 10 units	Arbitrary-direction modular network	[72]
Jiang *et al*. (2020)	TENG	Swing cylinder; air gap and flexible brushes	Forced motion and water wave	88 s swing; no loss after 400,000 cycles	Ultra-low-frequency durability	[69]
Wang *et al*. (2021)	TENG	Seven parallel S-TENG units with 70 layers in total inside a buoy	Wave basin; parametric tests	Max. I_{sc}: 20.91 μA; max. Q_{sc}: 2.22 μC	Illuminated a 12 W-rated LED	[74]
Wang *et al*. (2024)	TENG	Rolling mode; tunnel-grating electrodes	Lab and in-situ ocean	Peak: 185.4 W/(m³·Hz); RMS: 10.92 W/(m³·Hz)	Computing node; 0.8 km wireless link	[75]
Gai *et al*. (2025)	TENG	Adaptive dual turbine and phase-shifting TENG	Simulated wave environment	Crest factor 1.077; 400 V; 80 μA	Low-ripple output; commercial sensors	[77]
Chen *et al*. (2020)	Hybrid	Chaotic pendulum TENG–EMG	Laboratory water wave	TENG 15.21 μW; EMG 1.23 mW	LEDs; wireless transmission >300 m	[89]
Feng *et al*. (2021)	Hybrid	Soft-contact cylindrical swing TENG–EMG	Ultra-low-frequency water wave	n.r.	Soft contact reduces wear	[90]
Zhu *et al*. (2023)	Hybrid	Integrated PM–PTFE ball TENG–EMG	1 Hz ±30°; down to 0.2 Hz	TENG 13.77 W/m³; EMG 148.24 W/m³	Wireless sea-temperature buoy	[95]
Li *et al*. (2024)	Hybrid	Bidirectional turbine; planetary-gear TENG–EMG	1 Hz; stable at 0.25 Hz	TENG 115 mW; EMG 350 mW	Unidirectional rotation; monitoring	[97]
Zhang *et al*. (2024)	Hybrid	Pressure-difference turbine TENG–EMG	Laboratory wave	TENG 141.7 W/m³; EMG 400.0 W/m³	Self-powered marine IoT buoy	[98]
Jia *et al*. (2025)	Hybrid	Self-adaptive gyroscope TENG–EMG	Water tank	29.92 W/(m³·Hz) and 402.08 W/(m³·Hz)	Omnidirectional current monitoring	[99]
Wang *et al*. (2025)	Hybrid	Coral-inspired TENG–EMG sensor	Laboratory wave	EMG ~3 mW; wave height R^2 = 0.95	Wave height and direction telemetry	[102]
He *et al*. (2026)	TENG	Constant-voltage wave and wind TENG	Water wave and in-situ	31.2 W/m³ at 2 Hz; 0.68% decay after 2.33 million cycles	Regulated output; commercial sensors	[103]
Zhao *et al*. (2025)	Hybrid	Chaotic pendulum; tower TENG–EMG	Tank and open-sea	56.7 and 192.3 W/(m³·Hz)	Broadband capture; sea monitoring	[100]

Notes: n.r., not reported or not quantified. Values are reproduced with the authors' normalizations. Entries without a pendulum are contextual comparators and are not used to rank pendulum WECs. Absolute power, volume-normalized power density, and frequency-normalized power density are separate metrics; W/m³ and W/(m³·Hz) are not directly comparable and should not be compared without the excitation spectrum, device-volume definition, electrical load, and averaging method.

from different devices and test protocols [69,103] and should therefore not be treated as a common durability benchmark. Open-sea evidence remains rare, so high laboratory power density should be treated as a hypothesis for field performance rather than proof of autonomous operation.

3. NONLINEAR DYNAMICS FOR BROADBAND HARVESTING

3.1. From Linear Resonance to Nonlinear Broadband Harvesting

A lightly damped linear pendulum harvester responds strongly over a narrow frequency range near resonance. Nonlinear stiffness bends the frequency response toward lower frequencies in softening systems and toward higher frequencies in hardening systems. Near twice the natural frequency, parametric modulation above a threshold can destabilize the zero-motion state [25]. In bistable harvesters, distinct responses can coexist under the same excitation [26]. When the motion crosses the potential barrier, snap-through can produce large-amplitude oscillations between the wells [26,27]. Other response regimes include sustained rotation in parametrically excited pendulums [24] and chaotic motion in base-excited double pendulums [36]. Figure **11** summarizes the excitation modes and dynamical analysis of pendulum harvesters, illustrates how their responses vary with

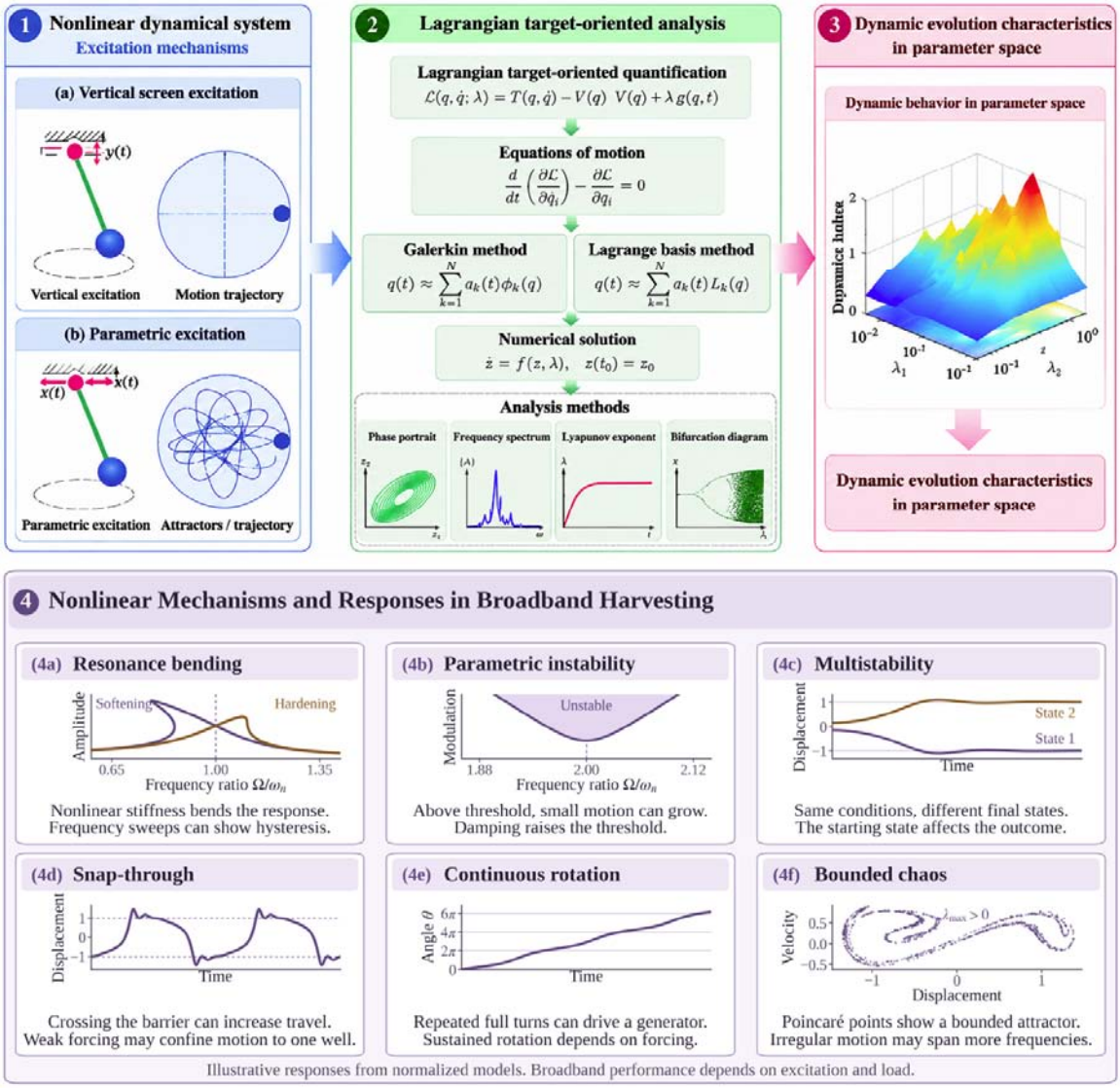


Figure 11: Analysis route for the nonlinear dynamics of pendulum harvesters and the six response mechanisms that enlarge the operational domain, namely resonance bending, parametric instability, multistability, snap-through, continuous rotation, and bounded chaos.

system parameters, and uses representative responses to explain the nonlinear mechanisms and motion regimes relevant to broadband energy harvesting. The usable harvesting bandwidth depends on the power delivered to the load under the specified excitation conditions.

3.2. Parametric Excitation, Rotation, and Multistability

When vertical or attitude motion modulates the effective gravitational restoring term, the pendulum follows a Mathieu-type equation and parametric instability can occur when the excitation frequency is close to twice the natural frequency of the relevant mode. Rotational orbits generally generate larger and more continuous relative velocity than small oscillations, but coexistence with low-energy attractors makes start-up sensitive to initial conditions and wave history [16-19,21-24]. Reid *et al*. compared surge, heave, and dynamic-tilt excitation across pendulum orientations: direct excitation produced peak power near resonance, parametric excitation near twice the natural frequency, and sufficiently large dynamic tilt enabled a response over frequencies approaching zero at the cost of a lower peak [25]. This bandwidth–peak-power trade-off is more informative than a single resonance curve.

Frequency tuning is necessary because a compact gravitational pendulum is usually too stiff for dominant ocean-wave periods. A counterweight can reduce the effective restoring moment without increasing length; magnetic negative stiffness can further soften the potential and introduce a controlled bistable region. Recent work combines both mechanisms to move compact-pendulum resonance toward the wave band while widening the usable response [28]. Tuning must be bounded by static stability and clearance constraints: excessive negative stiffness enlarges the low-energy basin or drives impacts, and a heavy

counterweight can compromise hull metacentric stability.

Multistability should therefore be analyzed probabilistically. Bifurcation diagrams identify solution branches, but basin stability and transition probability under stochastic excitation determine whether a desirable attractor is reachable. Magnetic rolling-pendulum studies show how well depth and excitation jointly control coexisting periodic and chaotic solutions [26]. Time-varying potential wells offer another mechanism: temporary barrier reduction promotes snap-through, after which the barrier is restored to retain large-amplitude motion [27]. For design, these maps should be computed jointly with generator torque and end-stop loads.

3.3. Electromechanical Coupling and Damping

Electrical extraction appears mechanically as speed-dependent torque, cogging, rectifier nonlinearity, and storage-voltage-dependent damping. Weak coupling yields large motion but little useful charge; excessive damping suppresses rotation and can trap the system in a low-energy orbit. The PTO should therefore be represented inside the nonlinear equation of motion rather than applied after a mechanical simulation. For EMGs, this requires flux linkage, coil resistance and inductance, rectifier loss, and load impedance. For TENGs, the state variables include transferred charge, electrode potential, capacitance as a function of displacement, leakage, and power-management switching [47,51,52,70,78-83].

Damping is also a control variable. Gu *et al*. used a digitally controlled variable-area hydraulic cylinder to adjust PTO resistance in real time and reported 37.04% more captured energy than a fixed-area cylinder, with approximately 95% average mechanical efficiency [42]. The same principle applies to electrical converters: load resistance, duty ratio, or generator current can be scheduled from estimated sea state and pendulum regime. Control energy and sensor overhead must be deducted; otherwise an adaptive strategy may improve gross capture while reducing net stored energy.

3.4. Experimental Validation

Validation should progress from component to system. Bench tests establish friction, cogging, electrical impedance, and repeatability. Forced-motion rigs map response to prescribed surge, heave, and tilt. Wave-basin tests then expose hydrodynamic coupling, directionality, and mooring effects under regular and irregular spectra. Finally, field trials reveal biofouling, sealing, corrosion, telemetry loss, storm survival, and the mismatch between forecast and encountered sea states. Scale conversion must distinguish Froude-scaled hydrodynamics from electrical and tribological processes that do not scale in the same way.

Recent studies illustrate the required progression. A 1:8.5 sealed pendulum buoy for met-ocean sensing measured angular speed, torque, voltage, and mooring tension in a basin with Froude interpretation [43]. Tank and open-sea tests of a high-entropy pendulum nanogenerator demonstrated broadband TENG–EMG conversion and wireless monitoring [100]. A coral-inspired hybrid reported self-powered wave-height sensing over 25–125 mm with $R^2 = 0.95$ [102], while a self-sustained observation buoy maintained a positive daily energy balance during a

Table 3: Gap-Cause-Response Matrix and Minimum Reporting Requirements for Self-Powered Observation Buoys

Gap	Root cause	Design response	Minimum evidence	Ref.
Spectral mismatch and directional sensitivity	Compact pendulum resonance exceeds wave peak; sea spectra and direction vary	Counterweight or magnetic softening; multi-axis geometry; adaptive PTO	Encountered spectrum; response map; bandwidth; start-up probability; net stored energy	[25,28,41,42]
Incomplete coupled prediction	Hull, pendulum, mooring, PTO and storage are solved sequentially	Time-domain fluid–mechanical–electrical co-simulation with measured losses	6-DOF motion; mooring loads; electrical state; parameter identification; uncertainty bounds	[33,39,41,45]
Non-comparable performance	Different volume definitions, loads, wave inputs, and normalizations	Common metrics and full test metadata	Geometry and mass; wave spectrum; scale; load; averaging window; W/m³ versus W/(m³·Hz); raw data	[57,75,76,95]
Limited field and lifecycle evidence	Short tests omit storms, corrosion, biofouling, wear and standby losses	Staged basin-to-sea validation; modular sealing; health monitoring	Duration; uptime; daily energy balance; failures; corrosion and wear; maintenance; sensor and telemetry duty cycle	[43,100,103, 104,106]

Recommended core metrics should be reported in separate bins: capture width or capture-width ratio where hydrodynamic input is known; absolute electrical output with peak, average, or RMS explicitly identified; volume- or frequency-normalized output with the active-volume definition; rectified and stored energy per sea state; start-up and attractor-transition probability; mechanical and electrical efficiency; quiescent power; observation availability; durability cycles; and field uptime.

three-week Yellow Sea deployment; its power-management unit had a reported quiescent demand of 0.74 mW [104]. These cases move evaluation from transducer peaks toward system availability, although they represent different devices and validation conditions. Earlier water-quality mapping work likewise linked triboelectric generation with real-time environmental sensing [105].

4. DESIGN FRAMEWORK FOR SELF-POWERED OBSERVATION BUOYS

4.1. Key Scientific Challenges

Four gaps dominate the transition from prototypes to dependable instruments: spectral mismatch, incomplete multiphysics coupling, non-comparable performance reporting, and insufficient lifecycle evidence. Table **3** links each gap to a design response and a minimum evidence package. The table is intended as a reporting checklist, not merely a summary of research needs.

4.2. Coupled Modeling and Hybrid Harvesting Framework

A defensible model contains five interacting layers. The environmental layer provides directional spectra, currents, wind, and extremes. The hydrodynamic layer resolves hull radiation, excitation, viscosity, and mooring loads. The mechanical layer captures nonlinear pendulum motion, friction, impacts, and internal coupling. The conversion layer represents EMG and TENG dynamics together with controllable PTO torque. The energy-service layer resolves rectification, storage, quiescent losses, sensing, computation, and communication. Closing the loop allows stored-energy state and sea-state estimates to modify PTO damping and observation duty cycle. The five-layer coupled framework and its supervisory feedback loop are illustrated in Figure **12**.

A representative implementation is the chaotic-pendulum hybrid nanogenerator of Zhao *et al.*, in which a tower-integrated TENG–EMG and charge-excitation circuit converted high-entropy wave motion in tank and sea trials [100]. Its significance is not only the reported peak density, but the co-location of nonlinear motion, hybrid conversion, power management, and wireless load. Future models should reproduce this complete energy path. Calibration can combine decay tests, forced-motion data, electrical impedance measurements, and Bayesian or physics-informed parameter estimation; predictions should include uncertainty bands instead of a single optimized trajectory.

4.3. Design Principles, Standardization, and Field Validation

Design should begin at the load. The daily energy demand is the sum of sensor warm-up, sampling, processing, storage, communications, localization, anti-fouling or heating functions, and power-management standby. A reserve margin must cover calm intervals and battery aging. The converter can then be sized against the joint distribution of sea state and mission demand. Net stored energy and observation availability are the primary objectives. Peak voltage, peak power, and hydrodynamic capture

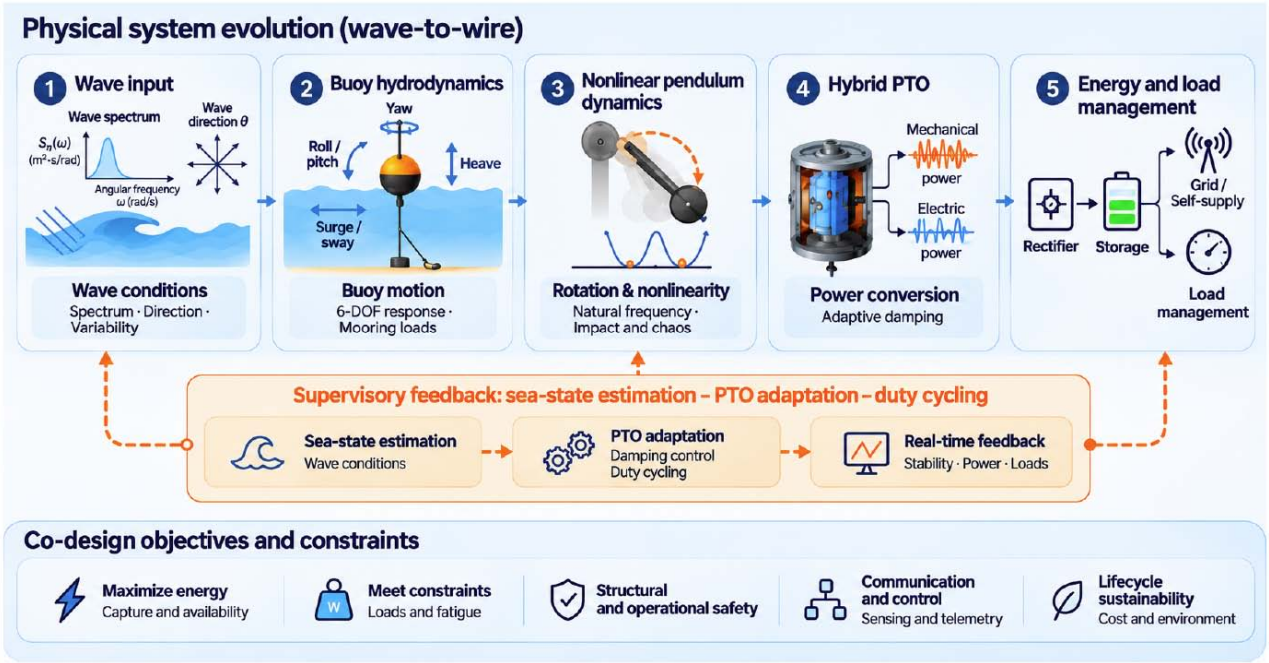


Figure 12: Five-layer coupled design framework for a pendulum-based self-powered marine observation buoy. Dashed arrows denote supervisory feedback from the energy-service layer to the PTO and mechanical response.

alone can be misleading when conversion losses, quiescent demand, or start-up thresholds dominate.

Mechanical co-design should preserve hull stability and serviceability. Place the pendulum close to the hull center where appropriate, verify metacentric height across storage state and flooding cases, and treat mooring stiffness as part of the excitation transfer path [41,45]. Bearings, gears, end stops, and cable routing require fatigue and wear assessment. Replaceable internal cartridges can separate maintenance of the converter from the certified hull. For hybrid PTOs, share the moving element but electrically isolate high-voltage TENG conditioning from the lower-voltage EMG and battery bus.

Reporting should follow Table **3**. Regular-wave response curves are insufficient: authors should provide irregular spectra, directionality, wave-height and period ranges, tank geometry, scale ratio, device mass and active volume, mooring configuration, electrical load, rectification and storage circuit, sampling interval, and uncertainty. Frequency-normalized and volume-normalized densities must be labeled explicitly and reported as separate metrics. Peak, average, and RMS values should not be combined without a stated conversion or averaging procedure. Durability should report cycle count together with motion amplitude, contact pressure, environment, and retained output. Whenever possible, anonymized time histories and analysis scripts should accompany the article.

Field qualification can use three gates. Gate 1 verifies sealing, mechanical clearance, and energy conversion during a short instrumented deployment. Gate 2 evaluates positive energy balance and data delivery across representative calm and energetic weeks. Gate 3 addresses seasonal endurance, storm survival, corrosion, biofouling, and maintainability. The three-week Yellow Sea demonstration provides an emerging system-level benchmark, but longer deployments and cross-site replication are still required [104]. Mooring loads and navigational risk should be included in the acceptance criteria, not treated as deployment details.

4.4. Sustainability and Future Perspectives

Sustainability must be evaluated over the complete service life. A compact harvester may avoid repeated battery-replacement voyages, but this benefit can be offset by short-lived tribological surfaces, difficult-to-recycle composites, rare-earth magnets, or oversized storage. Material selection should therefore combine conversion performance with fatigue, seawater compatibility, repairability, and end-of-life separation. Corrosion control should integrate coatings, galvanic isolation, sacrificial or impressed-current cathodic protection, and electrical grounding; energy-harvesting-assisted cathodic protection is an emerging option [106]. A lifecycle assessment should compare embodied carbon and replacement logistics with the avoided vessel fuel and discarded batteries. Life-cycle cost should include installation, mooring inspection, failure recovery, data loss, and decommissioning, not only prototype cost. These metrics connect marine energy research to the actual sustainability of an observation network.

Three directions are especially promising. First, reconfigurable stiffness and PTO control can move the operating regime as sea state and mission demand change. Second, modular arrays can separate high-energy capture from low-power sensing while retaining fault tolerance. Third, digital twins can assimilate motion, voltage, and storage data to estimate parameters, classify attractors, forecast energy availability, and schedule sensing. Physics-informed and uncertainty-aware learning is preferable to black-box optimization because field datasets are sparse and safety constraints are explicit. The control objective should remain interpretable: maximize observation value and net stored energy while respecting stability, fatigue, communication, and lifecycle limits.

5. CONCLUSIONS

Pendulum-based WECs provide a credible pathway to energy-autonomous marine observation because they package low-frequency inertial conversion within a sealed floating platform. The state of the art has expanded from single-axis electromagnetic pendulums to multi-axis, magnetic, triboelectric, and hybrid systems. Nonlinear effects—parametric excitation, rotation, multistability, snap-through, and bounded chaos—can increase bandwidth, but only when start-up probability, structural load, generator damping, and storage thresholds are considered together.

The literature reports advances in power density, adaptive PTO control, durability, and system integration, alongside persistent weaknesses in metric comparability and field evidence. A five-layer environmental–hydrodynamic–mechanical–conversion –energy-service framework is proposed to align device dynamics with sensing demand. Progress toward deployable infrastructure now depends less on isolated peak outputs and more on standardized irregular-wave testing, positive daily energy balance, sea trials lasting several weeks to multiple seasons, maintainable sealing and mooring, and lifecycle assessment. These priorities define the evidence needed to assess

whether miniature pendulum converters can become dependable components of sustainable ocean-observation networks.

CONFLICTS OF INTEREST

The authors declare no known competing financial interests or personal relationships that could have influenced the work reported in this paper.

AUTHOR CONTRIBUTIONS

Jiaze Kou and Qijian Feng: Conceptualization, Methodology, Literature curation, Visualization, Writing – original draft preparation.

Tiancong Zhao: Conceptualization, Supervision, Writing – review and editing, Funding acquisition.

FUNDING

This work was supported by the National Natural Science Foundation of China (52601580) and the China Postdoctoral Science Foundation (2025M774205, 2026T191074).

ABBREVIATIONS

CoG = center of gravity

DOF = degree of freedom

EMG = electromagnetic generator

IoT = Internet of Things

PTO = power take-off

RMS = root mean square

TENG = triboelectric nanogenerator

WEC = wave energy converter

REFERENCES

[1] Schiermeier Q, Tollefson J, Scully T, Witze A, Morton O. Energy alternatives: Electricity without carbon. Nature 2008; 454(7206): 816-823. https://doi.org/10.1038/454816a

[2] Kroger S, Law RJ. Sensing the sea. Trends Biotechnol 2005; 23: 250-256. https://doi.org/10.1016/j.tibtech.2005.03.004

[3] Observation ROV system. Available online: http://www.robosea.org/rov.html (accessed on 29 September 2026).

[4] Zhao T, Xu M, Xiao X, Ma Y, Li Z, Wang Z. Recent progress in blue energy harvesting for powering distributed sensors in ocean. Nano Energy 2021; 88: 106199. https://doi.org/10.1016/j.nanoen.2021.106199

[5] Tateson J, Jones A, Miller B, McGrath S, Beecroft T, O'Donnell D, Popay G. Real world issues in deploying a wireless sensor network for oceanography. In Proceedings of the Workshop on Real-World Wireless Sensor Networks, Stockholm, Sweden 2005.

[6] Xu G, Shen W, Wang X. Applications of wireless sensor networks in marine environment monitoring: a survey. Sensors 2014; 14: 16932-16954. https://doi.org/10.3390/s140916932

[7] Tollefson J. Power from the oceans: Blue energy. Nature 2014; 508: 302-304. https://doi.org/10.1038/508302a

[8] Scruggs J, Jacob P. Harvesting Ocean Wave Energy. Science 2009; 323: 1176-1178. https://doi.org/10.1126/science.1168245

[9] Khan J, Bhuyan G, Moshref A, Morison K, Pease JH, Gurney J. Ocean wave and tidal current conversion technologies and their interaction with electrical networks. In Proceedings of the 2008 IEEE Power and Energy Society General Meeting, 2008; pp. 1-8. https://doi.org/10.1109/pes.2008.4596550

[10] Falcão A.F.d.O. Wave energy utilization: A review of the technologies. Renew. Sustain. Energy Rev 2010; 14: 899-918. https://doi.org/10.1016/j.rser.2009.11.003

[11] Melikoglu M. Current status and future of ocean energy sources: A global review. Ocean Eng 2018; 148: 563-573. https://doi.org/10.1016/j.oceaneng.2017.11.045

[12] Westwood A. Ocean power: Wave and tidal energy review. Refocus 2004; 5: 50-55. https://doi.org/10.1016/S1471-0846(04)00226-4

[13] Hasan MH, Yang Y. Wave energy converters with rigid hull encapsulation: A review. Sustain. Energy Technol. Assess 2023; 57: 103273. https://doi.org/10.1016/j.seta.2023.103273

[14] Wang H, Sun J, Xi Z, Dai S, Xing F, Xu M. Recent progress on built-in wave energy converters: A review. J Mar Sci Eng 2024; 12: 1176. https://doi.org/10.3390/jmse12071176

[15] Davidson J, Nava V. Targeting the high-frequency tail of wave spectra for energy harvesting in marine sensor networks. Renew. Energy 2024; 237: 121550. https://doi.org/10.1016/j.renene.2024.121550

[16] Xu X, Wiercigroch M, Cartmell MP. Rotating orbits of a parametrically-excited pendulum. Chaos Solitons Fractals 2005; 23: 1537-1548. https://doi.org/10.1016/j.chaos.2004.06.053

[17] Garira W, Bishop SR. Rotating solutions of the parametrically excited pendulum. J Sound Vib 2003; 263: 233-239. https://doi.org/10.1016/S0022-460X(02)01435-9

[18] Yurchenko D, Alevras P. Stochastic Dynamics of a Parametrically base Excited Rotating Pendulum. Procedia IUTAM 2013; 6: 160-168. https://doi.org/10.1016/j.piutam.2013.01.018

[19] Yurchenko D, Naess A, Alevras P. Pendulum's rotational motion governed by a stochastic Mathieu equation. Probabilistic Eng Mech 2013; 31: 12-18. https://doi.org/10.1016/j.probengmech.2012.10.004

[20] Xu X, Pavlovskaia E, Wiercigroch M, Romeo F, Lenci S. Dynamic interactions between parametric pendulum and electro-dynamical shaker. ZAMM J Appl Math Mech 2007; 87: 172-186. https://doi.org/10.1002/zamm.200610311

[21] Lenci S, Brocchini M, Lorenzoni C. Experimental Rotations of a Pendulum on Water Waves. J Comput Nonlinear Dyn 2012; 7: 011007. https://doi.org/10.1115/1.4004547

[22] Alevras P, Yurchenko D. Stochastic rotational response of a parametric pendulum coupled with an SDOF system. Probabilistic Eng. Mech 2014; 37: 124-131. https://doi.org/10.1016/j.probengmech.2013.10.008

[23] Alevras P, Brown I, Yurchenko D. Experimental investigation of a rotating parametric pendulum. Nonlinear Dyn 2015; 81: 201-213. https://doi.org/10.1007/s11071-015-1982-8

[24] Yurchenko D, Alevras P. Parametric pendulum based wave energy converter. Mech Syst Signal Process 2018; 99: 504-515. https://doi.org/10.1016/j.ymssp.2017.06.026

[25] Reid M, Sorokin V, Aw K. Effects of pendulum orientation and excitation type on the energy harvesting performance of a pendulum based wave energy converter. Nonlinear Dyn 2024; 112: 20755-20769. https://doi.org/10.1007/s11071-024-10137-5

[26] Wang W, Wang J, Li B, Liu S, Li Z, Wei R. Bifurcation and multi-solution phenomena of a parametrically excited magnetic rolling pendulum bistable energy harvester. Nonlinear Dyn 2025; 113: 11093-11120. https://doi.org/10.1007/s11071-024-10796-4

[27] Fan Y, Niu MQ, Ghayesh MH, Amabili M, Chen L. Nonlinear vibration energy harvesting via parametric excitation: Snap-through with time-varying potential wells. Mech Syst Signal Process 2024; 220: 111625. https://doi.org/10.1016/j.ymssp.2024.111625

[28] Jiang S, Ding M, Lin W, Vijayasankar V, Truong BD, Zuo L. Counterweight and negative stiffness mechanisms for resonance tuning in pendulum-based wave energy converters. Proc Offshore Technology Conference 2026; OTC-37130-MS. https://doi.org/10.4043/37130-MS

[29] Zhou B, Zheng Z, Yao Y, He S, Jin P, Du H, Yang Y, Shi H. Wave energy converters: A comprehensive review of research progress, key challenges, and future trends. Appl Energy 2026; 413: 127722. https://doi.org/10.1016/j.apenergy.2026.127722

[30] Huang X, Zheng Z, Jin P, Zhou B, Zhang H. Numerical optimization and experimental study on the hybrid system of pendulum WEC and floating breakwater. Energy 2025; 331: 136914. https://doi.org/10.1016/j.energy.2025.136914

[31] Guo Q, Sun M, Liu H, Ma X, Chen Z, Chen T, Sun L. Design and experiment of an electromagnetic ocean wave energy harvesting device. In Proceedings of the 2018 IEEE/ASME International Conference on Advanced Intelligent Mechatronics, Auckland, New Zealand 2018. https://doi.org/10.1109/AIM.2018.8452264

[32] Li Y, Guo Q, Huang M, Ma X, Chen Z, Liu H, Sun L. Study of an Electromagnetic Ocean Wave Energy Harvester Driven by an Efficient Swing Body Toward the Self-Powered Ocean Buoy Application. IEEE Access 2019; 7: 129758-129769. https://doi.org/10.1109/ACCESS.2019.2937587

[33] Jiang X, Shi H, Cao F, Zhao Z, Li M, Chen Z. System analysis and experimental investigation of a pendulum-based wave energy converter. Ocean Eng 2023; 277: 114300. https://doi.org/10.1016/j.oceaneng.2023.114300

[34] Ding W, Song B, Mao Z, Wang K. Experimental investigations on a low frequency horizontal pendulum ocean kinetic energy harvester for underwater mooring platforms. J Mar Sci Technol 2015; 21: 359-367. https://doi.org/10.1007/s00773-015-0357-7

[35] Li M, Deng H, Zhang Y, Li K, Huang S, Liu X. Ultra-Low Frequency Eccentric Pendulum-Based Electromagnetic Vibrational Energy Harvester. Micromachines 2020; 11: 1009. https://doi.org/10.3390/mi11111009

[36] Kumar R, Gupta S, Ali SF. Energy harvesting from chaos in base excited double pendulum. Mech Syst Signal Process 2019; 124: 49-64. https://doi.org/10.1016/j.ymssp.2019.01.037

[37] Wojna M, Wijata A, Wasilewski G, Awrejcewicz J. Numerical and experimental study of a double physical pendulum with magnetic interaction. J. Sound Vib 2018; 430: 214-230. https://doi.org/10.1016/j.jsv.2018.05.032

[38] Wang Y, Lee CK. Dynamics and power generation of wave energy converters mimicking biaxial hula-hoop motion for mooring-less buoys. Energy 2019; 183: 547-560. https://doi.org/10.1016/j.energy.2019.06.135

[39] Crowley S, Porter R, Taunton DJ, Wilson PA. Modelling of the WITT wave energy converter. Renew Energy 2018; 115: 159-174. https://doi.org/10.1016/j.renene.2017.08.004

[40] Zhang Y, Wen Y, Han X, Zhang W, Gao F, Chen W. Gyroscopic wave energy converter with a self-accelerating rotor in WEC-glider. Ocean Eng 2023; 273: 113819. https://doi.org/10.1016/j.oceaneng.2023.113819

[41] Jiang X, Cao F, Shi H, Zhu K, Zhang C. Optimization of pendulum-based wave energy converter through mathematical approximation. Appl Energy 2025; 378: 124754. https://doi.org/10.1016/j.apenergy.2024.124754

[42] Gu Y, Lin Y, Li D, Lu X, Liu H, Sun Y. An integrated piston-variable digital-controlled hydraulic cylinder for pendulum wave energy converter. IEEE J Ocean Eng 2025; 50: 2135-2145. https://doi.org/10.1109/JOE.2025.3531959

[43] Shalaby A, Abd El-Latief ME, Shah A, Paredes R, Mi J, Datla R. Development and experimental investigation of a pendulum-based WEC for met-ocean sensing. Proc ASME IMECE 2025; IMECE2025-166654. https://doi.org/10.1115/IMECE2025-166654

[44] Khan A, Kuo E, Alahdal E, Kothari N, Patel M, Alam R. Design optimization and experimental validation of a pendulum-based WEC for autonomous ocean drones. Proc European Wave and Tidal Energy Conference 2025. https://doi.org/10.36688/ewtec-2025-1141

[45] Jiang X, Zhao C, Shi H, Johanning L. Hybrid mooring design for a pendulum-based wave energy converter. Mar Energy Res 2026; 3: 10014. https://doi.org/10.70322/mer.2026.10014

[46] Wang Z, Jiang T, Xu L. Toward the blue energy dream by triboelectric nanogenerator networks. Nano Energy 2017; 39: 9-23. https://doi.org/10.1016/j.nanoen.2017.06.035

[47] Wang Z. On Maxwell's displacement current for energy and sensors: the origin of nanogenerators. Mater Today 2017; 20: 74-82. https://doi.org/10.1016/j.mattod.2016.12.001

[48] Wang Z. Triboelectric nanogenerators as new energy technology and self-powered sensors - principles, problems and perspectives. Faraday Discuss 2014; 176: 447-458. https://doi.org/10.1039/C4FD00159A

[49] Wang S, Lin L, Wang Z. Triboelectric nanogenerators as self-powered active sensors. Nano Energy 2015; 11: 436-462. https://doi.org/10.1016/j.nanoen.2014.10.034

[50] Wang Z. Nanogenerators, self-powered systems, blue energy, piezotronics and piezo-phototronics - A recall on the original thoughts for coining these fields. Nano Energy 2018; 54: 477-483. https://doi.org/10.1016/j.nanoen.2018.09.068

[51] Wang Z. On the expanded Maxwell's equations for moving charged media system - General theory, mathematical solutions and applications in TENG. Materials Today 2022; 52: 348-363. https://doi.org/10.1016/j.mattod.2021.10.027

[52] Cheng T, Shao J, Wang Z. Triboelectric nanogenerators. Nat. Rev. Methods Primers 2023; 3: 39. https://doi.org/10.1038/s43586-023-00220-3

[53] Yang X, Xu L, Lin P, Zhong W, Bai Y, Luo J, Chen J, Wang Z. Macroscopic self-assembly network of encapsulated high-performance triboelectric nanogenerators for water wave energy harvesting. Nano Energy 2019; 60: 404-412. https://doi.org/10.1016/j.nanoen.2019.03.054

[54] Wang J, Pan L, Guo H, Zhang B, Zhang R, Wu Z, Wu C, Yang L, Liao R, Wang Z. Rational Structure Optimized Hybrid Nanogenerator for Highly Efficient Water Wave Energy Harvesting. Adv. Energy Mater 2019; 9: 1802892. https://doi.org/10.1002/aenm.201802892

[55] Liang X, Jiang T, Liu G, Xiao T, Xu L, Li W, Xi F, Zhang C, Wang Z. Triboelectric Nanogenerator Networks Integrated with Power Management Module for Water Wave Energy Harvesting. Adv Funct Mater 2019; 29: 1807241. https://doi.org/10.1002/adfm.201807241

[56] Shi Q, Wang H, Wu H, Lee C. Self-powered triboelectric nanogenerator buoy ball for applications ranging from environment monitoring to water wave energy farm. Nano Energy 2017; 40: 203-213. https://doi.org/10.1016/j.nanoen.2017.08.018

[57] Rodrigues C, Nunes D, Clemente D, Mathias N, Correia JM, Rosa-Santos P, Taveira-Pinto F, Morais T, Pereira A, Ventura J. Emerging triboelectric nanogenerators for ocean wave energy harvesting: state of the art and future perspectives. Energy Environ Sci 2020; 13: 2657-2683. https://doi.org/10.1039/D0EE01258K

[58] Tian J, Chen X, Wang Z. Environmental energy harvesting based on triboelectric nanogenerators. Nanotechnology 2020; 31: 242001. https://doi.org/10.1088/1361-6528/ab793e

[59] Liang X, Jiang T, Liu G, Feng Y, Zhang C, Wang Z. Spherical triboelectric nanogenerator integrated with power management module for harvesting multidirectional water wave energy. Energy Environ Sci 2020; 13: 277-285. https://doi.org/10.1039/C9EE03258D

[60] Xu L, Pang Y, Zhang C, Jiang T, Chen X, Luo J, Tang W, Cao X, Wang Z. Integrated triboelectric nanogenerator array based on air-driven membrane structures for water wave energy harvesting. Nano Energy 2017; 31: 351-358. https://doi.org/10.1016/j.nanoen.2016.11.037

[61] An J, Wang Z, Jiang T, Liang X, Wang Z. Whirling-Folded Triboelectric Nanogenerator with High Average Power for Water Wave Energy Harvesting. Adv Funct Mater 2019; 29: 1904867. https://doi.org/10.1002/adfm.201904867

[62] Zhong W, Xu L, Yang X, Tang W, Shao J, Chen B, Wang Z. Open-book-like triboelectric nanogenerators based on low-frequency roll-swing oscillators for wave energy harvesting. Nanoscale 2019; 11: 7199-7208. https://doi.org/10.1039/c8nr09978b

[63] Liang X, Jiang T, Feng Y, Lu P, An J, Wang Z. Triboelectric Nanogenerator Network Integrated with Charge Excitation Circuit for Effective Water Wave Energy Harvesting. Adv Energy Mater 2020; 10: 2002123. https://doi.org/10.1002/aenm.202002123

[64] Li X, Tao J, Wang X, Zhu J, Pan C, Wang Z. Networks of High Performance Triboelectric Nanogenerators Based on Liquid-Solid Interface Contact Electrification for Harvesting Low-Frequency Blue Energy. Adv Energy Mater 2018; 8: 1800705. https://doi.org/10.1002/aenm.201800705

[65] Tang W, Jiang T, Fan F, Yu A, Zhang C, Cao X, Wang Z. Liquid-Metal Electrode for High-Performance Triboelectric Nanogenerator at an Instantaneous Energy Conversion Efficiency of 70.6%. Adv Funct Mater 2015; 25: 3718-3725. https://doi.org/10.1002/adfm.201501331

[66] Zhang C, Liu L, Zhou L, Yin X, Wei X, Hu Y, Liu Y, Chen S, Wang J, Wang Z. Self-Powered Sensor for Quantifying Ocean Surface Water Waves Based on Triboelectric Nanogenerator. ACS Nano 2020; 14: 7092-7100. https://doi.org/10.1021/acsnano.0c01827

[67] Zhang Q, He M, Pan X, Huang D, Long H, Jia M, Zhao Z, Zhang C, Xu M, Li S. High performance liquid-solid tubular triboelectric nanogenerator for scavenging water wave energy. Nano Energy 2022; 103: 107810. https://doi.org/10.1016/j.nanoen.2022.107810

[68] Wang H, Feng M, Wang W, Wang W, Meng J, Liu Y, Wang Q, Wang D. Fluorine-free coating-based droplet triboelectric nanogenerators for highly efficient energy harvesting. J Mater Chem A 2024; 12: 4727-4738. https://doi.org/10.1039/D3TA07103K

[69] Jiang T, Pang H, An J, Lu P, Feng Y, Liang X, Zhong W, Wang Z. Robust Swing-Structured Triboelectric Nanogenerator for Efficient Blue Energy Harvesting. Adv Energy Mater 2020; 10: 2000064. https://doi.org/10.1002/aenm.202000064

[70] Chen P, An J, Cheng R, Shu S, Berbille A, Jiang T, Wang Z. Rationally segmented triboelectric nanogenerator with a constant direct-current output and low crest factor. Energy Environ Sci 2021; 14: 4523-4532. https://doi.org/10.1039/D1EE01382C

[71] Wang X, Niu S, Yin Y, Yi F, You Z, Wang Z. Triboelectric Nanogenerator Based on Fully Enclosed Rolling Spherical Structure for Harvesting Low-Frequency Water Wave Energy. Adv Energy Mater 2015; 5: 1501467. https://doi.org/10.1002/aenm.201501467

[72] Xu M, Zhao T, Wang C, Zhang S, Li Z, Pan X, Wang Z. High Power Density Tower-like Triboelectric Nanogenerator for Harvesting Arbitrary Directional Water Wave Energy. ACS Nano 2019; 13: 1932-1939. https://doi.org/10.1021/acsnano.8b08274

[73] Lin Z, Zhang B, Guo H, Wu Z, Zou H, Yang J, Wang Z. Super-robust and frequency-multiplied triboelectric nanogenerator for efficient harvesting water and wind energy. Nano Energy 2019; 64: 103908. https://doi.org/10.1016/j.nanoen.2019.103908

[74] Wang H, Fan Z, Zhao T, Dong J, Wang S, Wang Y, Xiao X, Liu C, Pan X, Zhao Y, Xu M. Sandwich-like triboelectric nanogenerators integrated self-powered buoy for navigation safety. Nano Energy 2021; 84: 105920. https://doi.org/10.1016/j.nanoen.2021.105920

[75] Wang Y, Du H, Yang H, Xi Z, Zhao C, Qian Z, Chuai X, Peng X, Yu H, Zhang Y, Li X, Hu G, Wang H, Xu M. A rolling-mode triboelectric nanogenerator with multi-tunnel grating electrodes and opposite-charge-enhancement for wave energy harvesting. Nat Commun 2024; 15: 6834. https://doi.org/10.1038/s41467-024-51245-5

[76] Jiang Y, Liang X, Jiang T, Wang Z. Advances in triboelectric nanogenerators for blue energy harvesting and marine environmental monitoring. Engineering 2024; 33: 204-224. https://doi.org/10.1016/j.eng.2023.05.023

[77] Gai Y, Jin B, Wang E, Bai Y, Jiang X, Sheng T, Yang X, Liu Z, Jiang Y, Li Z. Adaptive dual turbine triboelectric nanogenerator toward self-powered marine buoy. Nano Energy 2025; 144: 111356. https://doi.org/10.1016/j.nanoen.2025.111356

[78] Wang J, Wu C, Dai Y, Zhao Z, Wang A, Zhang T, Wang Z. Achieving ultrahigh triboelectric charge density for efficient energy harvesting. Nat Commun 2017; 8: 88. https://doi.org/10.1038/s41467-017-00131-4

[79] Liu W, Wang Z, Wang G, Liu G, Chen J, Pu X, Xi Y, Wang X, Guo H, Hu C, Wang Z. Integrated charge excitation triboelectric nanogenerator. Nat Commun 2019; 10: 1426. https://doi.org/10.1038/s41467-019-09464-8

[80] Liu Y, Liu W, Wang Z, He W, Tang Q, Xi Y, Wang X, Guo H, Hu C. Quantifying contact status and the air-breakdown model of charge-excitation triboelectric nanogenerators to maximize charge density. Nat Commun 2020; 11: 1599. https://doi.org/10.1038/s41467-020-15368-9

[81] Wang H, Xu L, Bai Y, Wang Z. Pumping up the charge density of a triboelectric nanogenerator by charge-shuttling. Nat Commun 2020; 11: 4203. https://doi.org/10.1038/s41467-020-17891-1

[82] Bai Y, Xu L, Lin S, Luo J, Qin H, Han K, Wang Z. Charge Pumping Strategy for Rotation and Sliding Type Triboelectric Nanogenerators. Adv Energy Mater 2020; 10: 2000605. https://doi.org/10.1002/aenm.202000605

[83] Wu H, Wang S, Wang Z, Zi Y. Achieving ultrahigh instantaneous power density of 10 MW/m² by leveraging the opposite-charge-enhanced transistor-like triboelectric nanogenerator (OCT-TENG). Nat Commun 2021; 12: 5470. https://doi.org/10.1038/s41467-021-25753-7

[84] Xi F, Pang Y, Liu G, Wang S, Li W, Zhang C, Wang Z. Self-powered intelligent buoy system by water wave energy for sustainable and autonomous wireless sensing and data transmission. Nano Energy 2019; 61: 1-9. https://doi.org/10.1016/j.nanoen.2019.04.026

[85] Wang X, Wen Z, Guo H, Wu C, He X, Lin L, Cao X, Wang Z. Fully Packaged Blue Energy Harvester by Hybridizing a Rolling Triboelectric Nanogenerator and an Electromagnetic Generator. ACS Nano 2016; 10: 11369-11376. https://doi.org/10.1021/acsnano.6b06622

[86] Hong H, Yang X, Cui H, Zheng D, Wen H, Huang R, Liu L, Duan J, Tang Q. Self-powered seesaw structured spherical buoys based on a hybrid triboelectric-electromagnetic

nanogenerator for sea surface wireless positioning. Energy Environ Sci 2022; 15: 621-632. https://doi.org/10.1039/d1ee02549j

[87] Zhang C, Yuan W, Zhang B, Yang O, Liu Y, He L, Wang J, Wang Z. High Space Efficiency Hybrid Nanogenerators for Effective Water Wave Energy Harvesting. Adv Funct Mater 2022; 32: 2111775. https://doi.org/10.1002/adfm.202111775

[88] Wen Z, Guo H, Zi Y, Yeh MH, Wang X, Deng J, Wang J, Li S, Hu C, Zhu L, Wang Z. Harvesting Broad Frequency Band Blue Energy by a Triboelectric-Electromagnetic Hybrid Nanogenerator. ACS Nano 2016; 10: 6526-6534. https://doi.org/10.1021/acsnano.6b03293

[89] Chen X, Gao L, Chen J, Lu S, Zhou H, Wang T, Wang A, Zhang Z, Guo S, Mu X, Wang Z, Yang Y. A chaotic pendulum triboelectric-electromagnetic hybridized nanogenerator for wave energy scavenging and self-powered wireless sensing system. Nano Energy 2020; 69: 104440. https://doi.org/10.1016/j.nanoen.2019.104440

[90] Feng Y, Liang X, An J, Jiang T, Wang Z. Soft-contact cylindrical triboelectric-electromagnetic hybrid nanogenerator based on swing structure for ultra-low frequency water wave energy harvesting. Nano Energy 2021; 81: 105625. https://doi.org/10.1016/j.nanoen.2020.105625

[91] Saadatnia Z, Asadi E, Askari H, Esmailzadeh E, Naguib HE. A heaving point absorber-based triboelectric-electromagnetic wave energy harvester: An efficient approach toward blue energy. Int J Energy Res 2018; 42: 2431-2447. https://doi.org/10.1002/er.4024

[92] Chen J, Guo H, Liu G, Wang X, Xi Y, Javed M, Hu C. A fully-packaged and robust hybridized generator for harvesting vertical rotation energy in broad frequency band and building up self-powered wireless systems. Nano Energy 2017; 33: 508-514. https://doi.org/10.1016/j.nanoen.2017.01.052

[93] Wang P, Pan L, Wang J, Xu M, Dai G, Zou H, Dong K, Wang Z. An Ultra-Low-Friction Triboelectric-Electromagnetic Hybrid Nanogenerator for Rotation Energy Harvesting and Self-Powered Wind Speed Sensor. ACS Nano 2018; 12: 9433-9440. https://doi.org/10.1021/acsnano.8b04654

[94] Liu L, Shi Q, Lee C. A novel hybridized blue energy harvester aiming at all-weather IoT applications. Nano Energy 2020; 76: 105052. https://doi.org/10.1016/j.nanoen.2020.105052

[95] Zhu C, Wu M, Liu C, Xiang C, Xu R, Yang H, Wang Z, Wang Z, Xu P, Xing F, Wang H, Xu M. Highly Integrated Triboelectric-Electromagnetic Wave Energy Harvester toward Self-Powered Marine Buoy. Adv Energy Mater 2023; 13: 2301665. https://doi.org/10.1002/aenm.202301665

[96] Lu Z, Zhao L, Fu H, Yeatman E, Ding H, Chen L. Ocean wave energy harvesting with high energy density and self-powered monitoring system. Nat Commun 2024; 15: 6513. https://doi.org/10.1038/s41467-024-50926-5

[97] Li T, Wang X, Wang K, Liu Y, Li C, Zhao F, Yao Y, Cheng T. Bidirectional rotating turbine hybrid triboelectric-electromagnetic wave energy harvester for marine environment monitoring. Adv Energy Mater 2024; 14: 2400313. https://doi.org/10.1002/aenm.202400313

[98] Zhang C, Yang S, Dai X, Tu Y, Du Z, Wu X, Huang Y, Fan J, Hong Z, Jiang T, Wang Z. Hybridized triboelectric-electromagnetic nanogenerators for efficient harvesting of wave energy for self-powered ocean buoy. Nano Energy 2024; 128: 109929. https://doi.org/10.1016/j.nanoen.2024.109929

[99] Jia S, Yang X, Feng W, Liu L, Zhao L, Wu L, Li S, Zuo W, Tang Q, Jiang T, Wang Z. Self-adaptive gyroscope-structured hybrid triboelectric-electromagnetic buoy system for real-time ocean currents monitoring. Small 2025; 21: 2501073. https://doi.org/10.1002/smll.202501073

[100] Zhao T, Li Z, Niu B, Xie G, Shangguan L, Zhang M, Zhu Y, Ma Y, Hu C, Li Y. A pendulum-based nanogenerator for high-entropy wave energy harvesting. Nat Commun 2025; 16: 5480. https://doi.org/10.1038/s41467-025-60443-8

[101] Gao L, Xu X, Han H, Yang W, Zhuo R, Wei Q, Deng Q, Hu N. A broadband hybrid blue energy nanogenerator for smart ocean IoT network. Nano Energy 2024; 127: 109697. https://doi.org/10.1016/j.nanoen.2024.109697

[102] Wang T, Guo Z, Jin H, Li Y, Liu B, Liu J, Xu G, Xu P, Xu M. A coral-inspired and fully self-powered wave monitoring system based on hybridized triboelectric-electromagnetic nanogenerator. Sens Actuators A Phys 2025; 387: 116451. https://doi.org/10.1016/j.sna.2025.116451

[103] He W, Yan W, Chen P, Li X, Zhao S, Li Z, Chen B, Jiang Y, Jiang T, Wang Z. A hybrid blue energy harvesting device based on constant-voltage triboelectric nanogenerator. Adv Funct Mater 2026; 36: e74644. https://doi.org/10.1002/adfm.74644

[104] Li Y, Tang T, Zhao H, Sun L, Zha F, Liu H. A self-sustained and self-sensing ocean observation buoy: System integration and in-situ sea trial. Ocean Eng 2026; 355: 125089. https://doi.org/10.1016/j.oceaneng.2026.125089

[105] Bai Y, Xu L, He C, Zhu L, Yang X, Jiang T, Nie J, Zhong W, Wang Z. High-performance triboelectric nanogenerators for self-powered, in-situ and real-time water quality mapping. Nano Energy 2019; 66: 104117. https://doi.org/10.1016/j.nanoen.2019.104117

[106] He J, Wang X, Wang M, Zhou H, Nan Y, Cui S, Zhang T, Yang L. Arch Shaped Triboelectric Nanogenerator for Wave Energy Harvesting and Corrosion Protection. Advanced Materials 2026; 38: e23290. https://doi.org/10.1002/adma.202523290

https://doi.org/10.65904/3083-0850.2026.01.07

© 2026 Kou *et al*.
This is an open access article licensed under the terms of the Creative Commons Attribution License (http://creativecommons.org/licenses/by/4.0/) which permits unrestricted use, distribution and reproduction in any medium, provided the work is properly cited.